Chinese Journal of Polymer Science Vol. 33, No. 4, (2015), 576–586

Chinese Journal of Polymer Science
© Chinese Chemical Society
Institute of Chemistry, CAS
Springer-Verlag Berlin Heidelberg 2015

The Crystallization Behavior of Biodegradable Poly(butylene succinate) in the Presence of Organically Modified Clay with a Wide Range of Loadings*

Jing-bin Chen, Jia-zhuang Xu, Huan Xu, Zhong-ming Li, Gan-ji Zhong** and Jun Lei**
College of Polymer Science and Engineering and State Key Laboratory of Polymer Materials Engineering, Sichuan University, Chengdu 610065, China

Abstract The crystallization behavior of poly(butylene succinate) (PBS) nanocomposites with a wide range of contents of clays was revealed. It was of interest to find that the crystallization rate of PBS was accelerated obviously at relatively low contents of clays; while a retarded crystallization kinetics and a decreased crystallinity of PBS were found in the nanocomposites with higher clay contents. Two interplaying effects existed in the nanocomposites, *i.e*., a suppression effect of clays on nucleation and a templating effect of clays on crystal growth, were clarified to contribute to this intriguing crystallization behavior.

Keywords: Poly(butylene succinate); Clay; Crystallization kinetics; Biodegradable.

Electronic Supplementary Material Supplementary material is available in the online version of this article at http://dx.doi.org/10.1007/s10118-015-1608-0

INTRODUCTION

A great wealth of investigations have established that nanocomposites incorporated with nanoclays present significantly improved physical/chemical properties, such as chemical stability[1], mechanical performances[2, 3], gas barrier[4, 5] and thermal properties[6]. For example, the oxygen permeability of pullulan decreased by orders of magnitude when it was incorporated with ~17 vol% of nanoclays[7]. The storage modulus of poly(L-lactic acid) containing 15 wt% nanoclays could be increased by 61.4% compared to that of the neat one[8]. Toward the fabrication of high-performance nanocomposites, clay-induced crystallization of polymer matrix is receiving increasing interest, mainly due to the direct dependence of bulk performances on the crystalline morphology and crystallinity (X_c) of the polymer. Qu *et al*. found that the presence of clays profoundly altered the crystallization kinetics of natural rubber, which made an obvious contribution to the tensile strength[9]. It is of great interest to observe the significantly enhanced impact toughness by the elaborate control in preferential formation of β-form isotactic polypropylene in the presence of clays[10–12]. Therefore, understanding the role of clays in tailoring the crystallization behavior as well as crystalline morphology has a special place in the field of manufacturing clay-based nanocomposites.

* This work was financially supported by the National Natural Science Foundation of China (Nos. U1162131 and 51473101), China Postdoctoral Science Foundation (Nos. 2012M521691 and 2014T70868), the Specialized Research Fund for the Doctoral Program of Higher Education (No. 20120181120101) and the Fundamental Research Funds for the Central Universities.
** Corresponding authors: Gan-ji Zhong (钟淦基), E-mail: ganji.zhong@scu.edu.cn
Jun Lei (雷军), E-mail: leijun@scu.edu.cn
Received July 23, 2014; Revised August 28, 2014; Accepted September 13, 2014
doi: 10.1007/s10118-015-1608-0

It has been revealed that clays usually act as effective nucleating agents for various semi-crystalline polymers[13–15]. For instance, the crystallization temperature of poly(butylene terephthalate) containing 5 wt% clays increased to 193.5 °C from 175.1 °C for neat poly(butylene terephthalate) during the non-isothermal crystallization at a cooling rate of 10 K/min[16]. As a response to the effective nucleation effect of clays, the spherulitic sizes of polymer matrix dramatically decreased[17–20]. Moreover, clays can lead to a large change of polymer crystallization kinetics. Even at a low clay content, it is normal to observe the evidently enhanced crystallization kinetics for the polymer matrix, essentially resulting from the nucleating effect of clays[21–24]. Benson *et al*. reported that the introduction of 1 wt% clays could increase the crystallization rate of syndiotactic polystyrene up to 3 times at the isothermal crystallization temperature of 240 °C[15]. However, the crystallization kinetics is featured by a downtrend as high contents of clays are added[21, 25]. It is primarily a result of the restricted crystal growth by the clay platelets[21, 24], eventually overcoming the nucleation activity of clays. From this perspective, the polymer composite loaded a high content of clays tends to exhibit huge differences in the crystalline morphology from that incorporated with a small amount of clays.

Poly(butylene succinate) (PBS), one of the most promising biopolymers, is characterized by a series of renowned merits including, but not limited to, desirable biodegradability, easy melt processability, and excellent thermal and chemical resistance[26]. The performance dwarves of PBS (such as poor stiffness, weak gas barrier and slow biodegradation), however, are frequently encountered in various end-use applications[27–29]. Many efforts have demonstrated the addition of clays holds the potential in overcoming these weaknesses of PBS[30–32]. It was revealed that the composites containing high contents of clays generally showed higher modulus and better gas barrier performances, compared to those incorporated with low contents of clays[33, 34]. Unfortunately, the crystallization behavior of PBS/clay composites, which represents great importance in understanding the structure-properites relationship, is rarely investigated. From the existing literatures, Phua *et al*. and Lim *et al*. reported the nonisothermal crystallization behavior of PBS/clay composites, and the crystallization rate of PBS was almost unchanged by the addition of clays[31, 35, 36]. Im *et al*. explored the isothermal crystallization kinetics of PBS at a clay loading of 2 wt%[37], in which largely improved crystallization rate was identified due to an increased active energy for nucleation and reduced energy for folding. Nevertheless, investigation on the crystallization behavior of PBS/clay nanocomposites is still limited for further understanding the reinforcement of clays on physical and mechanical properties of PBS, in particular with high content of clays.

In the present effort, we attempted to reveal the crystallization behavior of PBS/clay nanocomposites over a wide range of clay content (from 0.5 wt% to 40 wt%). The crystallization behavior was traced by differential scanning calorimetry (DSC), polarizing optical microscopy (POM), and 2D wide-angle X-ray diffraction (2D-WAXD). It was interestingly found that clays confined PBS nucleation and facilitated the growth of PBS crystals, and high loadings of clays decreased the X_c of PBS.

EXPERIMENTAL

Materials

PBS, model bionolle # 1001MD, is a commercial product of Showa Denko (Japan), which has a weight-average molecular weight and number-average molecular weight of 2.2×10^5 g/mol and 1.1×10^5 g/mol, respectively, and a melt flow rate of 1.6 g/10 min (190 °C, 2.16 kg). The organically modified clays (I.34TCN), which contain 30 wt% – 32 wt% organic modifier, were provided by Amcol International Corporation. The chemical structure of the specific organic modifier of the clays is $CH_3(CH_2)_{17}N(CH_3)[(CH_2CH_2OH)_2]^+$.

Preparation of PBS/Clay Nanocomposites

Prior to melt compounding, PBS was dried at 80 °C under vacuum for 24 h and the clays were dried at 105 °C under vacuum for 10 h. The melt mixing of PBS with clays was performed on a torque rheometer (XSS-300). The mixing was carried out for 10 min at 150 °C with the rotary speed of 50 r/min. The nanocomposites with different clay loadings, *i.e.*, 0.5 wt%, 1 wt%, 3 wt%, 5 wt%, 10 wt%, 20 wt%, and 40 wt% (the actual clay contents were about 0.35 wt%, 0.7 wt%, 2.1 wt%, 3.5 wt%, 7 wt%, 14 wt%, and 28 wt% when organic modifier

in the clays was overlooked) were prepared and noted as PBSC0.5, PBSC1, PBSC3, PBSC5, PBSC10, PBSC20, and PBSC40, respectively. All the samples were compression-molded at 150 °C and 10 MPa for 5 min to manufacture disks with a thickness of 1 mm and a diameter of 25 mm and films with a thickness of about 10 μm. These PBS/clay disks (or films) were used in the following characterizations.

Transmission Electronic Microscopy (TEM)

The morphology of the as-prepared PBS/clay nanocomposites were characterized by transmission electronic microscopy with an acceleration voltage of 200 kV (FEI Tecnai F20). Thin sections of the PBS nanocomposites with a thickness of ~80 nm for TEM observations were prepared by using a Leica EMUC6/FC6 microtome at –100 °C.

Differential Scanning Calorimetry (DSC)

DSC measurements were performed on a TA DSC Q2000 instrument. About 5 mg of each sample was heated to 150 °C at a heating rate of 20 K/min and held for 5 min to eliminate any thermal history. Then, the sample was cooled to 100 °C at a cooling rate of 30 K/min for isothermal crystallization. All the experiments were carried out in a nitrogen atmosphere. In order to reveal the growth geometry of crystals during isothermal crystallization, the Avrami equation was adopted as follows[38]:

$$\ln[-\ln(1-X(t))] = n\ln t + \ln k \tag{1}$$

where $X(t)$ was the relative crystallinity of a sample at a certain isothermal crystallization time (t); n and k were the Avrami exponent and the kinetic rate constant, respectively. Crystallization half-time ($t_{1/2}$), which represented the crystallization rate, was obtained by using equation (2) as follows:

$$t_{1/2} = [\ln 2/k]^{1/n} \tag{2}$$

Polarizing Optical Microscopy (POM)

Crystalline morphology of PBS and its nanocomposties was investigated by an Olympus BX51 polarizing optical microscope (Olympus Co., Tokyo, Japan) equipped with a MicroPublisher 3.3 RTV CCD. A Linkam CSS-450 high temperature optical stage was used to control the temperature with the accuracy of (± 0.1) K. The PBS/clay films were first melted at 150 °C for 5 min and then quenched to 100 °C for isothermal crystallization at a cooling rate of 30 K/min, which was same as the procedure of the isothermal crystallization described in DSC measurements.

Wide Angle X-ray Diffraction

The degree of clay exfoliation was measured by X-ray diffraction (XRD), which was taken on a Rigaku (Japan) diffractometer with Cu-Kα radiation of a wavelength of 0.1542 nm. This measurement was performed at a scanning rate of 3.6 (°)/min. The information of PBS crystals in the nanocomposites was characterized by 2D wide-angle X-ray diffraction (2D-WAXD). 2D-WAXD measurement was carried out at the beamline BC16B1 Shanghai Synchrotron Radiation Facility (SSRF, Shanghai, China), which was used to acquire 2D-WAXD images of PBS crystals. The wavelength of the X-ray was 0.124 nm. 2D-WAXD patterns were integrated azimuthally to obtain their corresponding diffraction profiles. Before testing, the PBS/clay disks were melted at 150 °C for 5 min and then isothermally crystallized at 100 °C in the Linkam CSS-450 high temperature optical stage, whose temperature procedures are consistent with DSC measurements. The X_c of PBS was calculated by

$$X_c = \frac{\sum A_{cryst}}{\sum A_{cryst} + \sum A_{amorp}} \tag{3}$$

where A_{cryst} and A_{amorp} represented the fitted areas of crystalline and amorphous phases of PBS, respectively.

RESULTS AND DISCUSSION

The Morphology of Clays in the Nanocomposites

To understand the origin of the effects of clays on polymer crystallization, it is instructive to reveal their morphologies in the nanocomposites. Figure 1 shows the XRD curves of neat PBS, neat clays, and their nanocomposites. The pristine clays show the characteristic diffraction peak of (001) plane at 4.65°, suggesting an interlayer spacing of 1.85 nm. This characteristic peak is not detected in the nanocomposites containing a clay content lower than 5 wt%, which indicates a good exfoliation of clays[39]. In the case of the nanocomposite loaded higher than 5 wt% of clays, the diffraction peak of the clays is observed, while the peak intensity significantly decreases and the interlayer spacing increases to 2.82 nm, consistent with a well intercalated structure of clays. The clays in the nanocomposites with either exfoliated structure or intercalated structure show at least 50% of increase in the spacing of clay platelets, which is much higher than about 12% of enhancement in the PBS/clay composites reported previously[40]. This is probably due to the good compatibility between fillers and matrix that facilitates the permeation of PBS chains into clay galleries in our study.

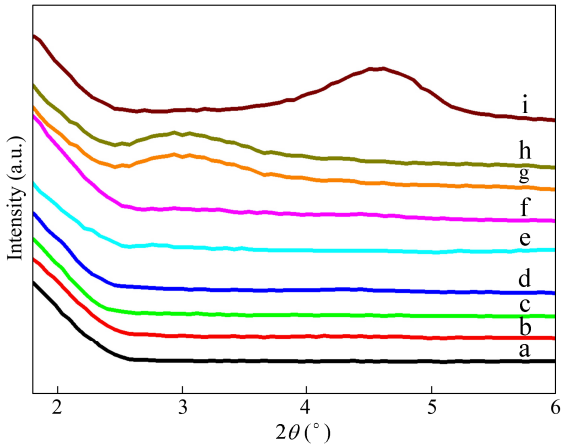


Fig. 1 XRD curves of (a) neat PBS, (b) PBSC0.5, (c) PBSC1, (d) PBSC3, (e) PBSC5, (f) PBSC10, (g) PBSC20, (h) PBSC40, and (i) neat clays (The wavelength of the X-ray is 0.1542 nm.)

Figure 2 presents the typical TEM micrographs of PBSC1, PBSC5 and PBSC20. One can clearly see that for all the three samples, clays are uniformly dispersed in PBS without evident agglomerations or large tactoids. The exfoliation degree of clays shows an apparent dependence on clay content. In the case of low clay contents, *e.g.*, PBSC1, the majority of clays are embedded in PBS matrix in the form of individual platelets, suggesting the quite exhaustive exfoliation; this is in good accordance with the result obtained from the XRD analysis. However, by increasing the clay content, instead of exfoliated structure, clays show hybrid structures consisting of intercalation and exfoliation structures, and the proportion of completely exfoliated clays tends to reduce with clay content. It is rational to deduce that the process of clay exfoliation initiates by the intercalation of PBS into clay galleries probably due to good miscibility between PBS and the modifier in this kind of clays[41], and subsequently the cohesive interactions between clay platelets can be further reduced by the further diffusion of PBS chains, which is expected to be favorable for the exfoliation of clays during mixing. As the clay content increases, the intercalation process could be suppressed due to confinement of chain diffusion, and meanwhile it is more likely to aggregate because of reduced distance of clay fillers, thus leading to the decreased exfoliation degree of clays.

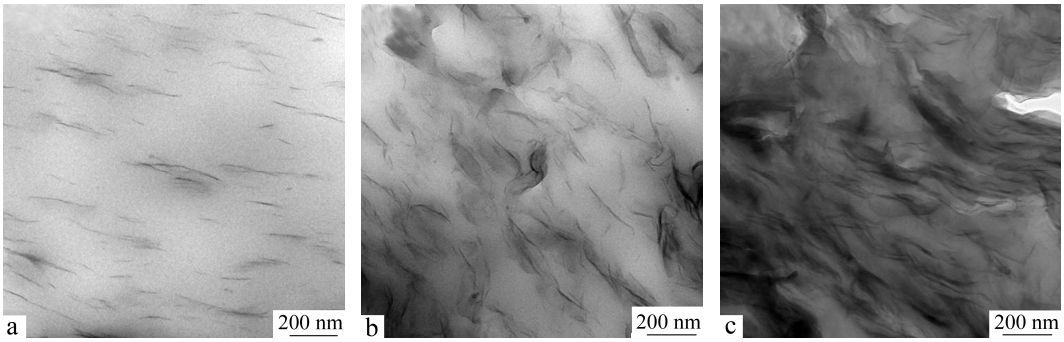


Fig. 2 TEM images of PBSC1 (a), PBSC5 (b) and PBSC20 (c)

Isothermal Crystallization Behavior of PBS/Clay Nanocomposites Measured by DSC

To explore the role of clays in the crystallization of PBS, the isothermal crystallization behavior of PBS/clay nanocomposites is investigated by DSC. Figure 3 shows the exothermic heat flow curves as a function of crystallization time for neat PBS and its nanocomposites isothermally crystallized at 100 °C. After crystallization induction periods, the exotherms diverge from the baseline, gradually approach the maximum peak along the time axis, and then back to a plateau; this represents the heat response throughout the PBS crystallization process. The peak time (representing the time when the maximum crystallization rate appears, t_{max}) can stand for the crystallization kinetics to some extent[38]. The smaller the t_{max} is, the faster the crystallization rate is. With increasing clay content, t_{max} first shifts to lower values. Unexpectedly, when the clay loading is beyond 5 wt%, t_{max} is prone to shift back to higher values compared to neat PBS, exhibiting a very interesting crystallization behavior.

The isothermal crystallization kinetics of PBS/clay nanocomposites are further analyzed by the Avrami equation (Eq. 1) in order to reveal the content depended crystallization kinetics in details. Figure 4 shows the plots of ln[−ln(1−X(t))] versus ln(t) for the isothermal crystallization of PBS/clay nanocomposites, in which the curves basically show linear variations. The Avrami exponent (n) indicating the nucleation process and growth dimension of PBS crystals can be calculated from the slopes of the curves (Fig. 5). The value of n gradually decreases with the clay content; *e.g.*, as the clay loading rises to 40 wt%, n reaches 2.46, suggesting a nearly-two-dimensional crystal growth mode. It has been reported earlier that the crystal growth dimension of polymers may reduce by increasing clay content[15, 41–44]. We assume the decreased n to the growth restriction of PBS crystal between crowded clays, where the growth dimension of PBS crystal may be two-dimensional[45]. Increasing the clay content, the clays become more compact in PBS matrix, thus leading to more obvious decline of n.

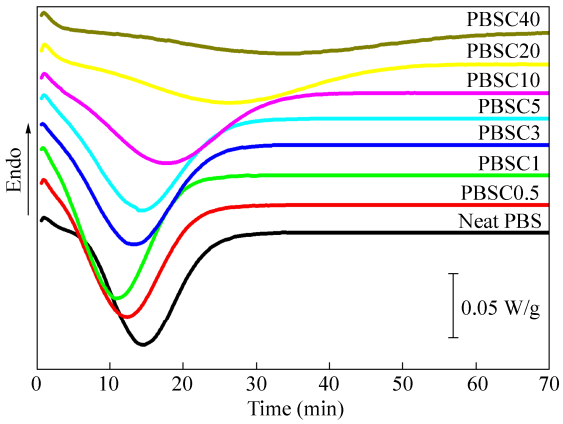


Fig. 3 Heat flow curves of the neat PBS and its clay nanocomposites during isothermal crystallization at 100 °C

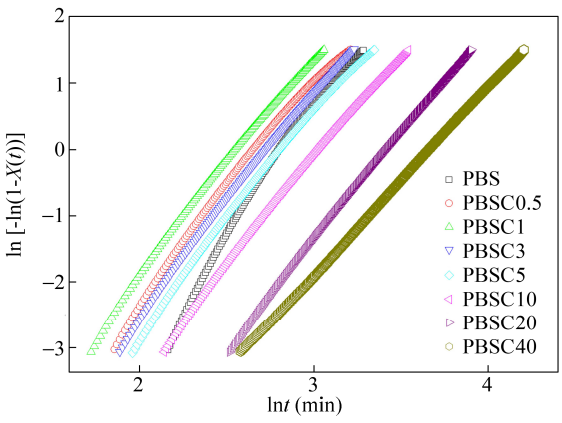


Fig. 4 Avrami plots for the neat PBS and PBS/clay nanocomposites during isothermal crystallization at 100 °C

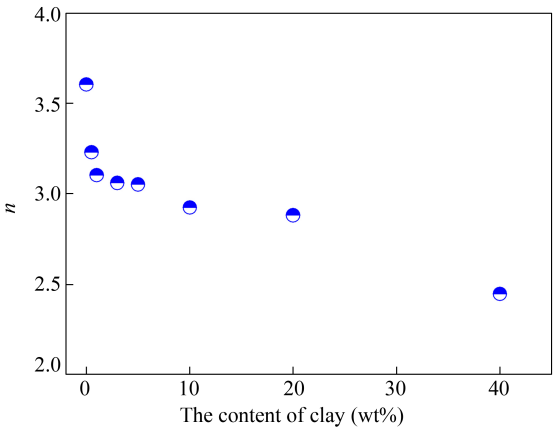


Fig. 5 The values of n of the neat PBS and its clay nanocomposites isothermally crystallized at 100 °C

According to Eq. (2), $t_{1/2}$, which is indicative of crystallization rate, is calculated. As shown in Fig. 6, the $t_{1/2}$ value decreases at first and then increases with the increase of clay loadings. Adding small amounts of clays to PBS, *i.e.*, 0.5 wt%, leads to a reduction in $t_{1/2}$, and the reduction becomes more obvious with increasing the clay content up to 1 wt%. As the clay loading rises from 1 wt% to 5 wt%, $t_{1/2}$ increases, but it is still lower than that of neat PBS, which suggests that PBS/clay nanocomposites reveal the fastest crystallization rate at a clay loading of 1 wt%. Additionally, PBSC5 shows almost the same $t_{1/2}$ value to neat PBS, implying 5 wt% clays is the transition loading for the crystallization kinetics of PBS from promoted crystallization to restricted one. Further increasing the clay content to higher than 5 wt%, the nanocomposites show larger $t_{1/2}$ values than that of neat PBS. For example, about 81% increase in $t_{1/2}$ from 15.0 to 27.1 min appears upon addition of 20 wt% clays. This means that relatively high loadings of clays inhibit, rather than promote the overall crystallization rate of PBS. Similar results were also observed in other clay-based polymer composites that the crystallization rate of polymer matrix had a transition from acceleration to confinement with increasing clay content[22, 46, 47].

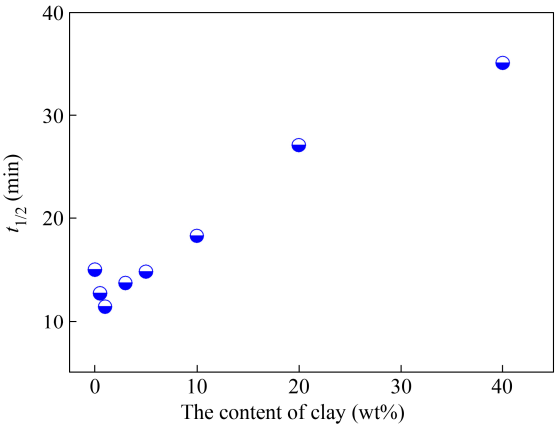


Fig. 6 Changes of crystallization half-time of the neat PBS and nanocomposites at isothermal crystallization temperature of 100 °C

We also investigate the isothermal crystallization behavior of PBS/clay nanocomposites at the temperatures of 95 °C and 105 °C, respectively (See Supporting Information). Obviously, the crystallization behavior of PBS/clay nanocomposites at the other two crystallization temperatures is quite similar to the phenomenon described at 100 °C. It is interesting to understand the details about the dependence of crystallization kinetics of

PBS on clay content. According to the works reported before[22, 48], the clays used herein seem to act as nucleating agents, leading to an acceleration of polymer crystallization at the low clay loadings; while at high loadings, the clays as crystallization retarders became more important, resulting in a deceleration of polymer crystallization. It is known that the overall crystallization rate was proportional to both the primary nucleation and the crystal/spherulite growth[24]. How can clays influence the nucleation and the crystal growth of PBS in the present work? It stimulates us to employ POM observation to investigate the crystallization behavior of PBS/clay nanocomposites with the goal of acquiring the mechanism on the crystallization of PBS at various clay loadings.

Isothermal Crystallization Behavior of PBS/Clay Nanocomposites Monitored by POM

Figure 7 illustrates typical polarized optical micrographs of the PBS and its nanocomposites during isothermal crystallization at 100 °C. It is obvious that at the same crystallization time, the number of PBS nucleation points decreases and the size of PBS spherulitic increases with the addition of clays, manifesting clays suppress PBS nucleation and facilitate PBS spherulitic growth. In accordance with Fig. 7, the nuclei densities and the growth rate of spherulite (G) of all the samples are obtained and presented in Fig. 8. Different from the previous report in the literatures, where clays usually acted as heterogeneous nucleating agents to increase the nuclei density of matrix on primary crystallization of a polymer[49, 50], the nuclei density of PBS remarkably reduces with adding clay into PBS, which can be exemplified by the decrease of 92% of the nuclei density (from 3510 mm^{-2} for neat PBS to 289 mm^{-2} for PBSC40). It primarily lies in the high miscibility between clays and PBS, which makes the lateral surface energy of clays in the nanocomposites close to that of PBS, consequently resulting in the attenuation or missing of nucleation effect of clays on PBS[42, 51]. It is worth mentioning that owing to the space limitation of clays, the motions of PBS chains are rigorously hindered to form crystal nuclei, which is suggested to be another main reason for the decrease of nuclei density caused by clays[52]. In addition, the nonisothermal crystallization of the samples measured by DSC also indicates that clays suppress the nucleation of PBS. As shown in Fig. S3 (See Supporting Information), in contrast to neat PBS, the onset crystallization temperature (T_0) and crystallization peak temperature (T_p) shift to lower temperatures in presence of clays and the excursion is more evident in the nanocomposites combining higher content of clays.

For the crystal growth after nucleation (Fig. 8b), G increases at first, and then shows little dependence on the clay content. As an example, the G value of PBSC3 is 1.22 μm/min, which is about 50% higher than that of neat PBS. This suggests that clays remarkably elevate the crystal growth of PBS, which is attributed to the templating effect of clay platelets on PBS crystal growth. Such a templating effect of clay platelets on polymer crystal growth may lie in the strong interface interaction between polymer and clays, which makes the arrangements of polymer chains into the nuclei near the clay platelets preferentially and rapidly. As the clay content increases to higher than 3 wt%, though more clays are added to PBS, there may be no obvious increase in clay platelet areas for supporting crystal growth since the clay exfoliation degree decreases; this is responsible to the constant G value at relatively high clay contents.

Evidently, different from the situation reported in previous studies that clays serve as nucleating agents and retard the spherulite growth of polymers[22, 48], clays have completely opposite effects on the nucleation and the crystal growth of PBS. Herein, clays serve as nucleating inhibitors to suppress PBS nucleation, which shows confinement effect on the crystallization of PBS; however, clay platelets facilitate the spherulite growth of PBS, exposing promotion effect on PBS crystallization. The dependence of PBS crystallization rate on clay content intrinsically results from the competition between the promotion effect and the confinement effect. When the clay content is lower than 5 wt%, the promotion effect of clays is dominant; thus, the addition of clays results in an improvement on the overall crystallization rate of PBS. Once the clay content exceeds 5 wt%, the confinement effect of clays becomes a paramount factor in determining the PBS crystallization kinetics, exhibiting a significant decrease in crystallization rate compared with that of neat PBS.

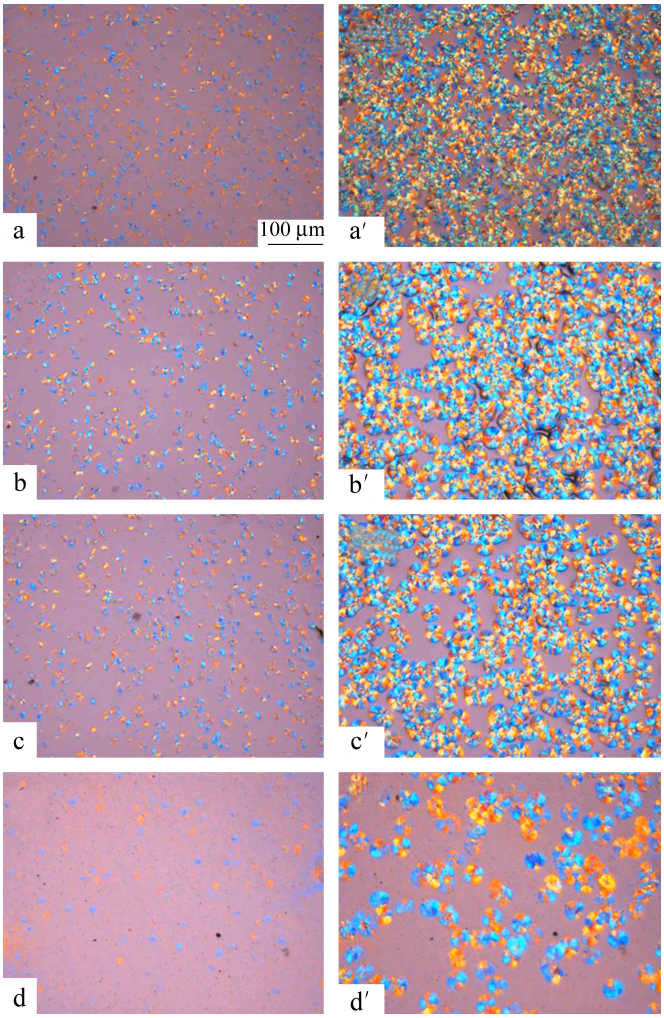


Fig. 7 Polarized optical micrographs of (a, a') neat PBS, (b, b') PBSC1, (c, c') PBSC5, and (d, d') PBSC20, respectively, during isothermal crystallization at 100 °C
The crystallization time of (a – d) is 8 min, and the crystallization time of (a' – d') is 20 min. All the samples have the same magnification.

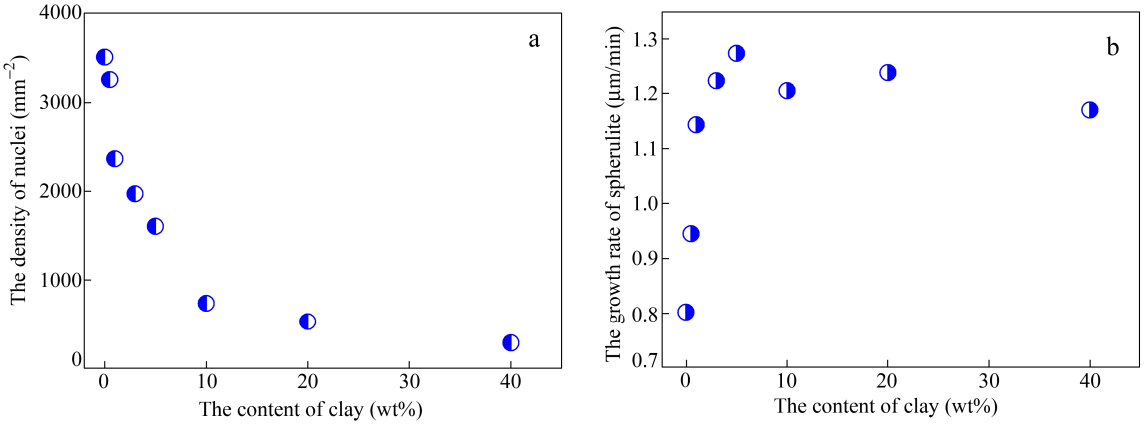


Fig. 8 The nuclei density (a) and spherulite growth rate (b) of PBS/clay nanocomposites as a function of clay content

Crystalline Structure and Morphology of PBS/Clay Nanocomposites

Besides the crystallization rate, the crystalline structure and morphology of PBS/clay nanocomposites are explored by 2D-WAXD measurements in order to obtain more insights into the influences of clays on PBS crystallization. Before the measurement, the PBS/clay disks were first melted at 150 °C for 5 min and then isothermally crystallized at 100 °C in the Linkam CSS-450 high temperature optical stage. Figure 9 illustrates the 1D-WAXD curves of neat PBS and its nanocomposites according to their 2D-WAXD patterns. All the samples show diffraction peaks of the α-crystals of PBS with the strong peak intensity at 15.7° and 18.1° representing (020) and (110) reflections. The characteristic diffraction of PBS β-crystals is not detected, suggesting clays have no impact on the crystalline modification of PBS at this crystallization temperature (100 °C).

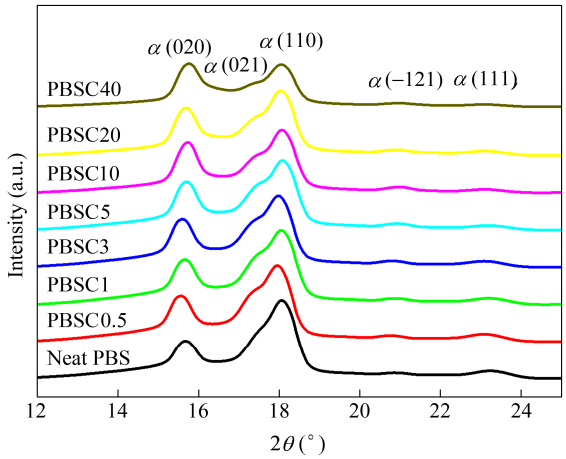


Fig. 9 Representative 1D-WAXD curves of the neat PBS and nanocomposites isothermally crystallized at 100 °C (The wavelength of the X-ray is 0.124 nm.)

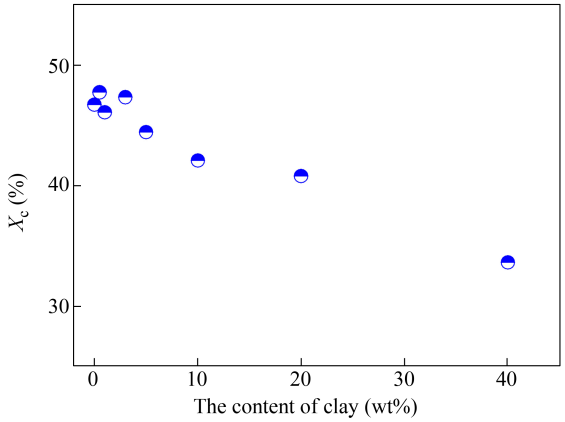


Fig. 10 The crystallinity of PBS/clay nanocomposites with different clay contents after isothermal crystallization at 100 °C

Figure 10 gathers the X_c of PBS/clay nanocomposites based on the 1D-WAXD curves. For nanocomposites with lower than 5 wt% of clays, the X_c of PBS remains almost invariable. While in the other samples, the X_c of PBS decreases markedly; *e.g.*, the X_c of PBSC40 is only 32.9%, revealing a 30% decrease compared to that of neat PBS. This can be explained by the space limitation of clays, which confines the crystallization of PBS[52].

Consequently, clays show complicated influences on the crystallization behavior of PBS, where clays not

only decrease the nuclei density and X_c of PBS, limit growth space for PBS crystal, but also facilitate the crystal growth rate of PBS. Based on these observations, we propose schematic diagrams in Fig. 11 to reveal the possible crystallization process of PBS/clay nanocomposites. That is, during melting mixture, due to high miscibility of organic compound in clay with PBS, an intercalation of PBS chains into clay galleries could happen and a dilute layer containing their miscible mixture of PBS and organic compound in the interface between clay and PBS matrix could form, which results in a suppressed nucleation in (and nearby) the clays, thereby nucleation tends to initiate in the PBS melt far from the clay galleries. As clay loading increases, the area favorable for nucleation decreases, leading to low nucleation rate at high loadings. As the crystal growth proceeds, PBS chains nearby the clay galleries arrange into the PBS nuclei preferentially and rapidly owing to the templating effect of clays.

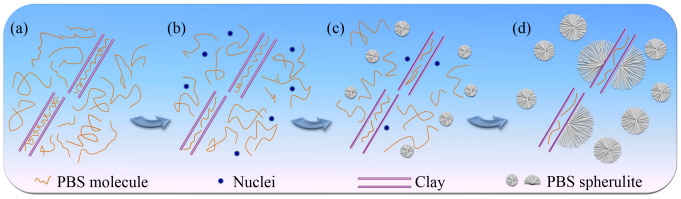


Fig. 11 Schematic diagrams of the crystallization process of PBS/clay nanocomposites at 100 °C, (a) the melt state, (b) PBS nucleation far from the clay galleries, (c) PBS nucleation nearby the clay galleries, (d) the growth of PBS crystals

CONCLUSIONS

We studied the crystallization behavior of PBS/clay nanocomposites over a wide range of clay contents with the assistance of POM, TEM, DSC and WAXD. Clays were well exfoliated in the nanocomposites with low clay contents and the exfoliation degree decreased with increasing clay content. The crystallization behavior of PBS was significantly affected by the loading of clay, but in an unusual way different from conventional nanofiller filled composites. Instead of heterogeneous nucleating agents, the clays used herein acted as nucleation inhibitors, which were attributed to the good compatibility between clays and PBS and the space limitation of clays. Moreover, the growth of PBS crystals was significantly improved compared to that of neat one due to a templating effect of clays on PBS crystal growth. By combining the nucleation and crystal growth, the bulk crystallization kinetics of PBS matrix was facilitated at low clay loadings and suppressed at high clay loadings, revealing a clay content dependence. In the crystallization process, the PBS chains were spatially confined by clays; this resulted in the decrease of PBS crystallinity.

ACKNOWLEDGMENTS We would like to express sincere thanks to the Shanghai Synchrotron Radiation Facility (SSRF, Shanghai, China), for the kind help on 2D-WAXD measurements.

REFERENCES

1 Vaia, R.A., Price, G., Ruth, P.N., Nguyen, H.T. and Lichtenhan, J., Appl. Clay Sci., 1999, 15(1): 67
2 Zhang, Q., Wang, K., Men, Y. and Fu, Q., Chinese J. Polym. Sci., 2003, 21(3): 359
3 Zhu, C.S., Kang, X., He, S.Q., Wang, L.Y. and Lu, L.Y., Chinese J. Polym. Sci., 2002, 20(6): 551
4 Kochumalayil, J.J., Bergenstråhle-Wohlert, M., Utsel, S., Wågberg, L., Zhou, Q. and Berglund, L.A., Biomacromolecules, 2012, 14(1): 84
5 Dunkerley, E. and Schmidt, D., Macromolecules, 2010, 43(24): 10536
6 Zhu, Y., Ma, H.Y., Tong, L.F. and Fang, Z.P., Chinese J. Polym. Sci., 2008, 26(6): 783
7 Introzzi, L., Blomfeldt, T.O., Trabattoni, S., Tavazzi, S., Santo, N., Schiraldi, A., Piergiovanni, L. and Farris, S., Langmuir, 2012, 28(30): 11206

8 Krikorian, V. and Pochan, D.J., Chem. Mater., 2003, 15(22): 4317
9 Qu, L., Huang, G., Liu, Z., Zhang, P., Weng, G. and Nie, Y., Acta Mater., 2009, 57(17): 5053
10 Dai, X., Zhang, Z., Wang, C., Ding, Q., Jiang, J. and Mai, K., Compos. Part A-Appl. Sci., 2013, 49: 1
11 Zhu, S., Chen, J., Zuo, Y., Li, H. and Cao, Y., Appl. Clay Sci., 2011, 52(1): 171
12 Varga, J. and Menyhárd, A., Macromolecules, 2007, 40(7): 2422
13 Miri, V., Elkoun, S., Peurton, F., Vanmansart, C., Lefebvre, J.M., Krawczak, P. and Seguela, R., Macromolecules, 2008, 41(23): 9234
14 Chen, B. and Evans, J.R., Macromolecules, 2006, 39(2): 747
15 Benson, S.D. and Moore, R.B., Polymer, 2010, 51(23): 5462
16 Chang, Y.W., Kim, S. and Kyung, Y., Polym. Int., 2005, 54(2): 348
17 Strawhecker, K. and Manias, E., Chem. Mater., 2003, 15(14): 844
18 Ma, J., Zhang, S., Qi, Z., Li, G. and Hu, Y., J. Appl. Polym. Sci., 2002, 83(9): 1978
19 Katoh, Y. and Okamoto, M., Polymer, 2009, 50(19): 4718
20 Nie, Y., Huang, G., Qu, L., Wang, X., Weng, G. and Wu, J., Polymer, 2011, 52(14): 3234
21 Lincoln, D.M., Vaia, R.A. and Krishnamoorti, R., Macromolecules, 2004, 37(12): 4554
22 Fornes, T. and Paul, D., Polymer, 2003, 44(14): 3945
23 Hwang, S., Khaydarov, A., Park, J., Yoo, E. and Im, S., Macromol. Res., 2011, 19(7): 699
24 Homminga, D., Goderis, B., Dolbnya, I., Reynaers, H. and Groeninckx, G., Polymer, 2005, 46(25): 11359
25 Homminga, D.S., Goderis, B., Mathot, V.B. and Groeninckx, G., Polymer, 2006, 47(5): 1630
26 Liu, W.G., Zhang, X.C., Li, G., Qi, R.R., Lu, J.Q., Hu, X.L., Luo, Y. and Jiang, P.K., J. Appl. Polym. Sci., 2013, 127(5): 3586
27 Tan, L.C., Chen, Y.W., Zhou, W.H., Ye, S.W. and Wei, J.C., Polymer, 2011, 52(16): 3587
28 Kuan, C.F., Ma, C.C.M., Kuan, H.C., Wu, H.L. and Liao, Y.M., Compos. Sci. Technol., 2006, 66(13): 2231
29 Zhang, K., Mohanty, A.K. and Misra, M., ACS Appl. Mater. Interfaces, 2012, 4(6): 3091
30 Okamoto, K., Sinha Ray, S. and Okamoto, M., J. Polym. Sci., Part B: Polym. Phys., 2003, 41(24): 3160
31 Phua, Y., Chow, W. and Ishak, Z.M., Express Polym. Lett., 2011, 5(2): 93
32 Someya, Y., Nakazato, T., Teramoto, N. and Shibata, M., J. Appl. Polym. Sci., 2004, 91(3): 1463
33 Sinha Ray, S., Okamoto, K. and Okamoto, M., Macromolecules, 2003, 36(7): 2355
34 Sinha Ray, S., Okamoto, K. and Okamoto, M., J. Appl. Polym. Sci., 2006, 102(1): 777
35 Phua, Y., Chow, W. and Ishak, Z.M., J. Thermoplast. Compos., 2011, 24(1): 133
36 Phua, Y., Lau, N., Sudesh, K., Chow, W. and Mohd, I.Z., Polym. Degrad. Stab., 2012, 97(17): 1345
37 Hwang, S.Y., Ham, M.J. and Im, S.S., Polym. Degrad. Stab., 2010, 95(8): 1313
38 Xu, D. and Wang, Z.G., Polymer, 2008, 49(1): 330
39 Martín, Z., Jiménez, I., Gómez-Fatou, M.A., West, M. and Hitchcock, A.P., Macromolecules, 2011, 44(7): 2179
40 Lim, S.K., Lee, J.J., Jang, S.G., Lee, S.I., Lee, K.H., Choi, H.J. and Chin, I.J., Polym. Eng. Sci., 2011, 51(7): 1316
41 Gopakumar, T., Lee, J., Kontopoulou, M. and Parent, J., Polymer, 2002, 43(20): 5483
42 Krikorian, V. and Pochan, D.J., Macromolecules, 2004, 37(17): 6480
43 Zhang, Q., Yu, M. and Fu, Q., Polym. Int., 2004, 53(12): 1941
44 Peneva, Y. and Minkova, L., Polym. Test., 2006, 25(3): 366
45 Xu, J.T., Wang, Q. and Fan, Z.Q., Eur. Polym. J., 2005, 41(12): 3011
46 Maio, E.D., Iannace, S., Sorrentino, L. and Nicolais, L., Polymer, 2004, 45(26): 8893
47 Wang, K., Liang, S., Deng, J.N., Yang, H., Zhang, Q., Fu, Q., Dong, X., Wang, D.J. and Han, C.C., Polymer, 2006, 47(20): 7131
48 Morales, A.R., de Paiva, L.B., Zattarelli, D. and Guimarães, T.R., Polímeros, 2012, 22(1): 54
49 Perez, C. and Alvarez, V.J., Appl. Polym. Sci., 2009, 114(5): 3248
50 Luduena, L.N., Vazquez, A. and Alvarez, V.A., J. Appl. Polym. Sci., 2008, 109(5): 3148
51 Krikorian, V. and Pochan, D.J., Macromolecules, 2005, 38(15): 6520
52 Sinha Ray, S. and Bousmina, M., Polymer, 2005, 46(26): 12430